This article has been published under the terms of the Creative Commons Attribution-Noncommercial 3.0 Unported License.
JPET Fast Forward. Published on May 17, 2011 as DOI: 10.1124/jpet.110.174466

JPET 174466

Exposure to an Environmental Neurotoxicant Hastens the Onset of ALS-Like Phenotype in hSOD1^{G93A} Mice: Glutamate-Mediated Excitotoxicity

Frank O. Johnson, Yukun Yuan, Ravindra K. Hajela, Alisha Chitrakar, Dawn M. Parsell, and William D. Atchison

Center for Integrative Toxicology (F.O.J., Y.Y., W.D.A.), Department of Pharmacology/Toxicology (F.O.J., Y.Y., R.K.H., D.M.P., A.C., W.D.A.) and Neuroscience Program (Y.Y., R.K.H., W.D.A.), Michigan State University, East Lansing, MI 48824

JPET Fast Forward. Published on May 17, 2011 as DOI: 10.1124/jpet.110.174466
This article has not been copyedited and formatted. The final version may differ from this version.

JPET 174466

Running Title: MeHg Facilitates Excitotoxicity in hSOD1^{G93A} Mice

Address all correspondence to:
Dr. William D. Atchison, Michigan State University
Department of Pharmacology and Toxicology
B331 Life Sciences Building,
East Lansing, MI 48824-1317
Phone: (517) 353-4947
Email: atchiso1@msu.edu.

Number of Text Pages: 23

Number of Tables: 1

Number of Figures: 7

Number of References: 60

Total Words in Abstract: 252

Total Words in Introduction: 825

Total Words in Discussion: 1890

Nonstandard Abbreviations: ALS, amyotrophic lateral sclerosis; AMPA, α-amino-3hydroxyl-5-methyl-4-isoxazole-propionate; CNQX, 6-cyano-7-nitroquinoxaline-2, 3-dione; EAAT, excitatory amino acid transporter; FALS, familial ALS; KA, kainic acid; MeHg, methylmercury; NAS, 1-naphthyl acetyl spermine trihydrochloride; NMDA, N-methyl-Daspartate; NXII, nucleus hypoglossal neurons; SALS, sporadic ALS; SOD1, Cu^{2+}/Zn^{2+}superoxide dismutase 1; TPEN, N,N,N',N'-tetrakis (pyridylmethyl) ethylenediamine

Recommended Section Assignment: Toxicology or Neuropharmacology

JPET Fast Forward. Published on May 17, 2011 as DOI: 10.1124/jpet.110.174466
This article has not been copyedited and formatted. The final version may differ from this version.

ABSTRACT

Mice expressing the human SOD1 gene mutation (hSOD1^{G93A}, G93A) were exposed to methylmercury (MeHg) at concentrations that did not cause overt motor dysfunction. We hypothesized that low concentrations of MeHg could hasten development of the Amyotrophic Lateral Sclerosis- (ALS) like phenotype in G93A mice. MeHg (1 or 3 ppm/day in drinking water) concentration-dependently accelerated the onset of rotarod failure in G93A, but not *wt* mice. At the time of rotarod failure, MeHg increased Fluo-4 fluorescence ($[Ca^{2+}]_i$), in soma of brainstem-hypoglossal nucleus. These motor neurons control intrinsic and some extrinsic tongue function, and exhibit vulnerability in bulbar-onset ALS. The AMPA/KA receptor antagonist CNQX reduced $[Ca^{2+}]_i$ in all G93A mice, irrespective of MeHg treatment. N-acetyl spermine, which antagonizes Ca^{2+}-permeable AMPA receptors, further reduced $[Ca^{2+}]_i$ more effectively in MeHg-treated than untreated G93A mice, suggesting that MeHg-treated mice have a greater Ca^{2+}-permeable AMPA receptor contribution. The non-Ca^{2+} divalent cation chelator N,N,N',N'-tetrakis (pyridylmethyl) ethylenediamine reduced Fluo-4 fluorescence in all G93A mice; FluoZin-(Zn^{2+} indicator) fluorescence was increased in all MeHg-treated mice. Thus in G93A mice Zn^{2+} apparently contributed measurably to the MeHg-induced effect. This is the initial demonstration of accelerated onset of ALS-like phenotype in a genetically-susceptible organism by exposure to low concentrations of an environmental neurotoxicant. Increased $[Ca^{2+}]_i$ induced by the G93A-MeHg interaction was apparently associated with Ca^{2+}-permeable AMPA receptors and may contribute to the hastened development of ALS-like phenotypes by subjecting motor neurons to excessive elevation of $[Ca^{2+}]_i$, leading to excitotoxic cell death.

JPET Fast Forward. Published on May 17, 2011 as DOI: 10.1124/jpet.110.174466
This article has not been copyedited and formatted. The final version may differ from this version.

INTRODUCTION

Gene-environmental interactions refer to phenotypic effects of environmental exposures on certain individuals due to genetic or epigenetic predisposition. These interactions putatively initiate or unmask signs of a disease and/or hasten its progression in susceptible individuals (Migliore and Coppedè, 2009). Such interactions have long been postulated to contribute to the etiology of neurodegenerative diseases such as Alzheimer's, Parkinson's Disease and possibly Amyotrophic Lateral Sclerosis (ALS) (Prasad et al., 1999; Mitchell, 2000; Swash, 2000; Migliore and Coppedè, 2009).This is based on the fact that demonstrable genetic links to these diseases have either not been identified or comprise only a small fraction of the reported cases. However, identifying contributory environmental triggers has been difficult, in part due to the long lag before display of clinical signs and the fact that exposure to an environmental "stressor" may not have been overt. No specific environmental exposure has yet been linked unequivocally to a given neurodegenerative disease. Thus, this hypothesis remains controversial, and for the most part untested.

ALS is a progressive, degenerative and fatal neurological disorder characterized by decreased skeletal muscle function as a result of loss of upper and/or lower motor neurons (Rowland and Shneider, 2001). Two general forms of ALS are widely recognized: familial (FALS) and sporadic (SALS). They present indistinguishable clinical signs and symptoms, which suggests that similar pathogenic pathways are involved. FALS accounts for 5-10% of all cases of ALS, whereas SALS makes up over 90% of the cases. However, lack of a clear identifiable genetic link to the vast majority of ALS cases makes the potential contribution of environmental exposure appear especially

relevant. Several gene mutations have been associated with FALS, including the superoxide radical scavenging enzyme Cu/Zn-superoxide dismutase -1 (SOD1) and recently TDP-43 (TAR DNA Binding Protein-43) and FUS (Fused in Sarcoma) or TLS (Translocated in Liposarcoma) (Kabashi et al., 2008; Sreedharan et al., 2008). These latter play a role in nucleic acid synthesis. Gene mutations including those in SOD1 have also been reported in a small percentage of SALS cases (Gruzman et al., 2007).

Recent evidence suggests that such a gene-environment interaction may contribute to the etiology of ALS. The 2006 report of the Institute of Medicine of the National Academy of Sciences (IOM, 2006) outlined potential risk factors for ALS, including head trauma, certain occupations and perhaps military service, with environmental exposures that facilitate excitotoxicity. Studies of Persian Gulf War veterans reported an increased incidence of ALS among returning veterans, with a much earlier age of onset, suggesting that exposure to some environmental factor triggered the disease or hastened its onset (Karsarkis et al., 1999; Haley, 2003; Horner et al., 2003).

Certain pesticides and heavy metals have been postulated most frequently as environmental risk factors for developing ALS (Mitchell, 2000). One such metal is mercury. Several isolated observations have been noted that are consistent with, but nonetheless circumstantial with respect to, effects of mercurials on motor neurons. Following ingestion, organic mercury compounds have been reported to concentrate in the cerebral cortex, brainstem (Møller-Madsen, 1991) and spinal cord (Arvidson 1992) - areas of the brain that are known to degenerate during ALS. Both Hg^{2+} and methylmercury (MeHg), the principal form of environmental mercury, produce ALS-like syndromes including disturbances of sensory/motor function and extremity weakness in

JPET Fast Forward. Published on May 17, 2011 as DOI: 10.1124/jpet.110.174466
This article has not been copyedited and formatted. The final version may differ from this version.

animals and human poisoning (Barber, 1978). Nonetheless, no cause and effect relationship has ever been established between ALS and exposure to any specific environmental toxicant.

The objective of the present study was to test the hypothesis of a gene-environment interaction in development of ALS-like phenotype using a genetically-susceptible animal. The model organism chosen was a well-described transgenic mouse that develops an ALSlike phenotype (Gurney et al., 1994; Brown, 1995). It over-expresses a mutated form of the human SOD1 gene in which a glycine for alanine substitution occurs (hSOD1 ^{G93A} - G93A). It is a commonly used and widely accepted animal model for study of both forms of ALS (see Benmohamed et al.,2010; Synofzik et al., 2010).

The model neurotoxicant chosen was MeHg. It was selected based on several criteria. The first was that it has been related at least circumstantially to ALS-like signs (Barber, 1978). The second was that it shared a common mode of action-glutamateinduced, Ca^{2+}-dependent neurotoxicity (See review by Allen et al., 2002; Limke et al., 2004; Grosskreutz et al., 2010)-with development of ALS. The third was that the primary target of the neurotoxicant not be on motor neurons, so that any effect caused was clearly due to an interaction as opposed to a primary effect of the compound. The rationale was that if a common toxic pathway contributed to expression of disease phenotype, it might be sufficient to provide a multi-hit form of damage (see review by Le et al., 2009) to the motor system, thereby hastening the onset of ALS phenotype, even if the target brain regions differed.

Glutamate-induced toxicity has been associated with cerebellar neurotoxicity to MeHg (Yuan and Atchison, 2007) and is commonly associated with the etiology of ALS.

Motor neuron dysfunction is not a primary effect commonly associated with exposure to MeHg. Neurotoxicity, instead, typically expresses in cerebellum and visual cortex (Bakir et al., 1973). Thus, this lack of normally expressed motor dysfunction should make MeHg a valuable agent with which to test for a gene-environment interaction in that development of ALS phenotype would not be a normal manifestation of MeHg neurotoxicity.

We report the role of increases in [Ca^{2+}] and [Zn^{2+}], coupled with greater sensitivity of Ca^{2+}-permeable AMPA receptors to MeHg toxicity leading to hastened development of hind limb paralytic phenotype in G93A mice.

MATERIALS AND METHODS

Chemicals and solutions. Fluo-4 NW was purchased from Invitrogen, Molecular Probes (Carlsbad, CA). α-Amino-3-hydroxyl-5-methyl-4-isoxazole-propionate (AMPA), kainic acid (KA), N-methyl-D-aspartate (NMDA), 1-naphthylacetyl spermine trihydrochloride (NAS), 6cyano-7-nitroquinoxaline-2,3-dione (CNQX), and 5-, N,N,N',N'-tetrakis (pyridylmethyl) ethylenediamine (TPEN) were all purchased from Sigma-Aldrich (St. Louis, MO). Methylmercuric chloride (MeHg) was purchased from ICN Biomedicals Inc. (Aurora, OH). Fluo-4 NW stocks (1X) were prepared by combining 5 ml of artificial cerebrospinal fluid (ACSF) and 100 µl of 250 µM probenecid (5 µM final concentration) to each vial of Fluo-4. Vials were then sonicated, solution aliquoted and stored in a foil-wrapped (eppendorf) container at -20°C. Stock solutions of chemicals were prepared as follows: NMDA and AMPA (10 mM) were dissolved in distilled water, filtered, aliquoted and kept in the freezer at -20°C. KA (10 mM) stock solution was prepared by adding 1-2 drops of 1N NaOH to the appropriate volume of distilled water prior to storage at -20°C. The corresponding chemicals were then included in the ACSF perfusate and aerated with 95% O_2/ 5% CO_2 at room temperature of 23-25°C, before (pre-drug) and during the experiments. MeHg stock solution, 500 ml of 20 mg/L concentration, was prepared by dissolving it in MilliQ® filtered water and stored at 4°C.

Oxygenated slicing solution contained (in mM): 125, NaCl; 2.5, KCl; 4, $MgCl_2$; 1.25; KH_2PO_4; 26, $NaHCO_3$; 1, $CaCl_2$ and 25, D-glucose (pH 7.35 - 7.4 when saturated with 95% O_2/5% CO_2 at room temperature of 22 - 25^{o}C). ACSF, in which all experiments were conducted, was identical in composition to the slicing solution, except that $MgCl_2$ was reduced to 1 mM and $CaCl_2$ was increased to 2 mM (Yuan and Atchison, 2007).

JPET Fast Forward. Published on May 17, 2011 as DOI: 10.1124/jpet.110.174466
This article has not been copyedited and formatted. The final version may differ from this version.

Some experiments, utilized 10 mM and 40 mM KCl to depolarize the plasma membrane. The composition of these solutions was otherwise identical to normal ACSF except that equimolar substitutions of K^+ for Na^+ were made to maintain osmolarity.

Breeding and PCR-Genotyping. All animal use and breeding protocols were approved by the Institutional Animal Care and Use Committee (IACUC) of Michigan State University and were carried out in accordance with the National Institute of Health (NIH) guidelines for the care and use of laboratory animals. Transgenic male mice hemizygous for the mutated human SOD1 gene, (stock #002726 [B6SJL-TgN ($SOD1^{G93A}$) 1Gur/J], Jackson Laboratory, Bar Harbor, ME) were used for breeding stock (Gurney et al., 1994). Tail snip DNA and PCR were used to confirm the presence of the $SOD1^{G93A}$ gene. Upon arrival of breeders, one heterozygote male was cohabitated with two B6SJLF1/J females (stock # 100012 Jackson Laboratory) in a 1:2 mating scheme. This design provided both sufficiently large litter numbers and a genetic pairing favorable for maintaining stable copy numbers of the hSOD1 mutation. Mice were housed and maintained in an AAALAC -accredited, climate-controlled facility. They were supplied free choice with Harlan Teklad #8640 feed and MilliQ® -filtered water. Pups were genotyped before weaning as previously described (Alexander et al., 2004).

Chronic MeHg Exposure. The exposure paradigm and time course of experimentation is depicted schematically in Figure 1. After weaning (PND 21) and genotyping, cohorts of male G93A and *wt* mice were randomly assigned to groups treated with 0, 1, or 3 ppm of MeHg. These concentrations were selected based on reported effects of low dose, lifetime exposure of MeHg on motor function and their ability to accumulate in

JPET Fast Forward. Published on May 17, 2011 as DOI: 10.1124/jpet.110.174466
This article has not been copyedited and formatted. The final version may differ from this version.

brain regions similar to those affected in ALS (Stern et al., 2001; Weiss et al., 2005). The MeHg dosing solution was diluted on a weekly basis by adding the appropriate quantity of stock concentration to 5 nM Na_2CO_3 buffering solution to produce 1-ppm and 3-ppm. Mice received MeHg freechoice *via* drinking water starting on PND29. This time point was selected to avoid any neurotoxic effects of MeHg on postnatal brain development which could have affected learning of the task independent of its effects on motor neuron degeneration. The 0 ppm control groups received the 5 nM-Na_2CO_3 drinking solution. Animal weights were recorded thrice weekly.

Total Tissue Mercury. Trunk blood (100 µl) and brainstem samples (0.1 g) were taken from G93A and 3-ppm *wt* mice at the onset of hind limb paralysis, typically at 3-4 mos of age. Untreated *wt* mice were culled at 3-4 mos. Samples were collected from 10 mice of each genotype and treatment group and stored at -20˚C until analyzed. Total Hg concentration was determined using cold-vapor atomic absorption spectrometry by the Diagnostic Center for Population and Animal Health, Michigan State University.

Rotarod Test. The time course of development of motor dysfunction associated with the ALS-like phenotype was tracked using a variable speed rotarod (diameter 3.175 cm, IITC, Life Science, Woodland Hills, CA). This is a simple test that depends on both CNS and peripheral neuromuscular function. While it is not specific for motor neuron function, it is easy to use, reliable, and a commonly accepted test of motor function. The inability of each mouse to maintain coordination and balance for 10 s at increasing speed (10-13 rpm in 10 s) heralds the irreversible and debilitating process of paralysis in this ALS mouse model. Beginning on PND50 (see Fig. 1), each mouse was trained on the

rotarod with three trials per day for 130 s each. Trials were spaced 10 min apart and training lasted for three consecutive days. The experimental phase was started on PND57 and continued for three consecutive days per week using similar parameters as the habituation phase described above. Rotarod performance was started on PND 50, 21 days following first exposure to MeHg as a precaution against potential developmental effects of MeHg which could affect task acquisition in this test (cf- Newland and Rasmussen, 2000; Newland et al., 2004; Bellum et al., 2007). This still permitted detection of hind limb dysfunction in the MeHg-treated G93A group well before the expected time of paralysis without MeHg, usually 120 days. “Failure” was scored if a mouse could not remain on the rotarod for at least 10 s for 2 of 3 consecutive trials on two consecutive days. Once a mouse failed the rotarod test, they were maintained with or without MeHg, dependent on the treatment group, until dysfunction was clearly evident in at least one hind limb. This interval was typically short- 2-3 days, reflecting the rapid progression of the hind limb dysfunction once it commenced.

Preparation of Adult Mouse Brainstem Slices. Brainstem slices were collected for a given mouse 2-3 days after the onset of rotarod failure (typically 3 - 4 mos old). They were used to test specifically for lower motor neuron function using *nucleus hypoglossus (NXII)* and Fluo-4 and/or FluoZin fluorescence confocal microscopy techniques and tissue Hg measurement as described below. NXII motor neurons control intrinsic and some extrinsic tongue function and are typically among the most affected muscles in both bulbar and spinal onset forms of ALS (DePaul et al., 1988). For all experiments, the mice were decapitated under deep CO_2 anesthesia; their brains were isolated quickly and immersed immediately in ice-cold slicing solution. Coronal

brainstem slices of 200 µm thickness were then collected and incubated in ACSF for a minimum of two hrs before being used for confocal microscopy studies.

Laser Scanning Confocal Microscopy. For divalent cation fluorescence measurement, slices were incubated at room temperature for 1-2 hr in ACSF containing Fluo-4 NW with or without 5 µM N,N,N',N'-tetrakis (pyridylmethyl) ethylenediamine (TPEN) (see below results). Hypoglossal cells (NXII) were visualized under a 10x objective fitted to a Leica DM LFSA (Leica Optics, Bannockburn, IL). NXII identification was based on its anatomical proximity to the central canal and vagus nerve. Fluo-4 and FluoZin fluorescence were measured in NXII motor neuronal soma using laser scanning confocal microscopy with a 40x water immersion objective (NA 0.75). Slices loaded with 1x Fluo-4 (no wash) and/or 5 µM FluoZin were excited by 488 nm argon laser light attenuated to 10%; emitted fluorescence was collected at 515 or 560 nm, respectively. Images (512 x 512 pixels, xyz scan mode) for FluoZin and/or Fluo-4 mediated fluorescence were collected before (predrug) and during perfusion with modified ACSF-containing 10 or 40 mM KCl. In addition, Fluo-4 mediated fluorescence was modulated with bath application of specific glutamate receptor agonists or antagonists. All experiments were carried out at room temperature of 23-25°C and data analysis was done offline using Leica software.

Statistical Analysis. Body weight and rotarod data were analyzed using two-way analysis of variance (ANOVA) with repeated measures. Total Hg concentration of blood and brainstem from an individual mouse was analyzed using one-way ANOVA. Normalized Fluo4 and/or FluoZin fluorescence (F/F_0) data were calculated after subtracting background fluorescence and by dividing the Ca^{2+} and/or Zn^{2+}-mediated

fluorescence stimulated by various pharmacological agents by the mean pre-drug Ca^{2+} fluorescence (ACSF only). The data were then analyzed using two-way ANOVA with repeated measures. If not indicated otherwise, values are expressed as mean ± standard error of the mean (SEM) and represent a minimum of 5-8 separate slices (1/mouse) for *in vitro* studies and 14 mice per treatment group for rotarod analyses. Significant mean differences were calculated using Dunnett's *posthoc* multiple comparison test. Statistical significance was set at $p<0.05$.

JPET Fast Forward. Published on May 17, 2011 as DOI: 10.1124/jpet.110.174466
This article has not been copyedited and formatted. The final version may differ from this version.

RESULTS

Total Tissue Mercury Concentration is Not Affected by Genotypes. MeHg accumulation in brainstem and blood following drinking water administration was measured (Table 1) to determine a) if MeHg treatment resulted in concentration-dependent increases in [Hg] as previously reported (Stern and Korn, 2001), and b) whether there was a differential accumulation of Hg by *wt* and G93A mice. Both G93A and *wt* mice exposed chronically to 1 or 3 ppm MeHg, accumulated approximately equivalent total Hg in blood and brainstem ($p>0.05$). Further there was no genotypic difference in Hg accumulation in blood or brainstem. Hg accumulation was, however, exposure concentration-dependent, ($p<0.05$).

Effects of MeHg Exposure on Body Weight. Overexpression of mutant human $Cu^{2+}/Zn^{2+}SOD1^{G93A}$ (G93A) genes in males typically generates smaller animals than *wt* littermates (Fig. 2A). Thus we wanted to test whether MeHg would further reduce body weight, perhaps contributing to a weakened state of the G93A mice or alternatively, reflecting effects on feeding behavior due to dysfunction of hypoglossal nerve innervated muscles. Mean body weight difference between G93A and treated *wt* at the start of rotarod training was 9% and at the symptomatic stages was 11%. The rate of incremental weight gain in treated *wt* was significantly ($p<0.05$) faster compared to treated or untreated G93A mice, with MeHg-treated *wt* mice attaining significantly greater body weight throughout the treatment period. For the G93A group, mice exposed to MeHg at either concentration, gained weight at least equal to or greater than untreated G93A mice. Body weights of untreated G93A and 3 ppm MeHg G93A were

JPET Fast Forward. Published on May 17, 2011 as DOI: 10.1124/jpet.110.174466
This article has not been copyedited and formatted. The final version may differ from this version.

similar at the start of exposure, however, on week 13 there was a significant ($p<0.05$) increase in weight gain in treated G93A mice that continued until week 15 (end stage of the disease). When compared to untreated G93A, mice exposed to 1 ppm MeHg exhibit a significantly ($p<0.05$) increased body weight starting already on week 9 until week 16 when they became paralyzed (end stage of the disease). G93A mice did gain weight, albeit at a slower rate, until the very end, at which point a larger increase was noted. This may reflect weights of animals that took a longer time to develop paresis. Over the entire experimental period, the body weight of untreated G93A mice did not increase appreciably. Shown in Panel B are comparative data for *wt* mice either unexposed or exposed to 3 ppm MeHg. There was little difference in either the rate of body weight gain, or the final weights achieved by *wt* mice in the presence of MeHg. Overall, MeHg exposure was not associated with a generalized metabolic decline, as reflected by body weight loss.

MeHg Exposure Hastened the Time to Onset of Rotarod Failure in G93A Mice. A rotarod test was used to track motor coordination and balance from pre-symptomatic (PND50) to symptomatic stages of ALS-like symptoms in both genotypes and treatment groups (Fig. 3). Normally, G93A mice developed paralytic hind limb phenotypes, as evidenced by failure to perform on the rotarod, which progressed to death in ~120 days, whereas their *wt* littermates exhibited no motor deficits and survived (Alexander et al., 2004). Exposure of *wt* mice to 3 ppm MeHg caused no decrement in rotarod performance over the duration of the observation period. They survived more than 120 days, at which point the experiment was terminated. In contrast, both untreated and MeHg-treated G93A mice exhibited time-dependent failure of motor coordination.

JPET Fast Forward. Published on May 17, 2011 as DOI: 10.1124/jpet.110.174466
This article has not been copyedited and formatted. The final version may differ from this version.

However, MeHg treatment significantly ($p<0.05$) hastened the time to onset of rotarod failure and hind limb paralysis in G93A mice. Exposure to either 1 or 3 ppm MeHg caused 50% of G93A mice to fail the test (median time) by 91 and 84 days, respectively, compared to 104 days in untreated G93A mice (Fig. 3A). This reduction was concentration-dependent ($p < 0.05$). At the point in the disease process at which 50% of males exposed to 3 ppm MeHg failed the rotarod test, only 21% of mice in the 1 ppm group failed, and no failures were recorded in either the untreated G93A control group or *wt* mice exposed to 3 ppm MeHg. The mean age to onset of ALS-like phenotype was also significantly ($p<0.05$) shortened at 1 or 3 ppm MeHg, compared to untreated G93A mice. Once failure in the rotarod test occurred, the time of progression (dragging of hind limb) to hind limb paralysis was significantly ($p<0.05$) shortened in G93A mice exposed to 3 but not 1 ppm MeHg when compared to untreated G93A controls.

Elevation of Intracellular Divalent Cations in G93A Mice at Time of Rotarod Failure. KCl-induced depolarization increased Fluo-4 fluorescence in both genotypes, ($F/F_0 >1$), with differential responses to MeHg treatment (Fig. 4A). At 10 mM, [KCl] significantly ($p<0.05$) augmented Fluo-4-fluorescence only in the 3 ppm MeHg-treated G93A mice, as compared to untreated G93A or *wt* (untreated and treated) slices. However, 40 mM [KCl] significantly ($p<0.05$) increased $[Ca^{2+}]_i$ in all treatment groups of the G93A mice, compared to *wt*. MeHg had no further effect to increase $[Ca^{2+}]_i$ above that in untreated G93A mice.

Fluo-4 binds not only Ca^{2+} but also other divalent cations such as Zn^{2+} which could artificially elevate the apparent increase in $[Ca^{2+}]_i$ fluorescence. MeHg releases a

JPET Fast Forward. Published on May 17, 2011 as DOI: 10.1124/jpet.110.174466
This article has not been copyedited and formatted. The final version may differ from this version.

non-Ca^{2+} divalent cation (Denny et al., 1993; Hare et al., 1993). In synaptosomes (Denny and Atchison, 1994) this was identified as Zn^{2+}. Additionally, in the G93A mice, impaired metal binding to SOD1 could result in an increase in intracellular Zn^{2+} (Beckman et al., 2001). As such, it was important to test for the possibility that more than one Fluo-4-chelatable cation contributed to the [KCl] depolarization-induced increase in Fluo-4 fluorescence. TPEN is a cell-permeant divalent cation chelator, which binds Zn^{2+} with high, and Ca^{2+} and Mg^{2+} with low affinity (Shmist et al., 2005). It does not bind MeHg (Hare et al., 1993). Incubation of brainstem slices for 2 hrs with Fluo-4 in the presence of 5 μM TPEN significantly ($p<0.05$) decreased [KCl]-induced Fluo-4 fluorescence compared to untreated slices (Fig. 4B). However, even in the presence of TPEN, Fluo-4 fluorescence was increased in a [KCl]-dependent manner. Consequently, we added TPEN to the Fluo-4 dye mix in all subsequent experiments.

Increased NXII Fluo-4 Fluorescence is Mediated Primarily by AMPA Receptors. To identify pharmacologically which types of glutamate receptors are responsible for the increased $[Ca^{2+}]_i$ in hypoglossal motor neurons, we compared effects of different glutamate receptor agonists on Fluo-4 fluorescence with or without MeHg treatment. Brainstem slices were stimulated sequentially with puff-application of NMDA, AMPA, or KA, each at 50 μM, for 120 s (Fig. 5). Neither NMDA nor KA significantly ($p>0.05$) increased mean normalized fluorescence in any genotype. Conversely, AMPA significantly ($p<0.05$) increased Fluo-4 fluorescence in both MeHg-treated and untreated G93A mice compared to *wt.* However, no further increase was seen upon exposure to MeHg as compared to untreated G93A mice ($p>0.05$).

JPET Fast Forward. Published on May 17, 2011 as DOI: 10.1124/jpet.110.174466
This article has not been copyedited and formatted. The final version may differ from this version.

AMPA receptor activation could result in increased Fluo-4 fluorescence if there was an increase in expression or activity of Ca^{2+}-permeable AMPA receptors (Kawahara et al., 2004; Tortarolo et al., 2006; Kwak et al., 2010). If such an effect occurred following MeHg exposure, it may not have been possible to detect an increase in MeHg-treated G93A hypoglossal motor neurons over that of untreated control using AMPA receptor agonists if the receptors had desensitized, thereby obscuring a potential effect. Consequently, treatment with an AMPA receptor antagonist was used in an attempt to attenuate the postsynaptic response. CNQX (20 μM) reduced mean normalized Fluo-4 fluorescence in both genotypes (F/F_0 <1) (Fig. 6). However, the effects were significantly ($p<0.05$) larger in the G93A group. MeHg-treatment did not further reduce $[Ca^{2+}]_i$ compared to untreated G93A slices ($p>0.05$).

AMPA receptors lacking GluR2 subunits comprise a subset of CNQX-sensitive receptors that are present in spinal motor neurons in humans (Kawahara et al., 2004) and G93A mice (Tateno et al., 2004; Rembach et al., 2004; Tortarolo et al., 2006). These receptors have a high Ca^{2+} conductance. We examined if Ca^{2+}-permeable AMPA receptors could contribute to increase Ca^{2+} in NXII neurons. NAS (50 μM) is a specific antagonist of Ca^{2+}-permeable AMPA receptors. It had little effect in *wt* as evidenced by normalized fluorescence >1 (Fig. 6). In comparison, it significantly ($p<0.05$) attenuated Fluo-4 fluorescence in G93A slices. Importantly, when compared to untreated G93A slices, normalized Fluo-4 fluorescence was further significantly ($p<0.05$) attenuated in MeHg treated G93A slices. The effect appeared to be MeHg-concentration dependent. Thus, NAS-sensitive, and presumably Ca^{2+}-permeable AMPA receptors, contribute significantly to MeHg-induced increase in Fluo-4 fluorescence in the G93A mice.

JPET Fast Forward. Published on May 17, 2011 as DOI: 10.1124/jpet.110.174466
This article has not been copyedited and formatted. The final version may differ from this version.

MeHg Elevation of Intracellular FluoZin Fluorescence in G93A and Wild-type Mice at the Time of Rotarod Failure. To test directly for a contribution of Zn^{2+} to the TPENsensitive component of Fluo-4 fluorescence, we used the Zn^{2+}-sensitive fluorophore FluoZin. Given the presence of Zn^{2+} in glutamatergic vesicles, KCl-induced depolarization could increase [Zn^{2+}] secondary to release of glutamate. KCl-induced depolarization increased FluoZin fluorescence in both genotypes, (F/F_0 >1), with differential responses to MeHg treatment (Fig. 7). At 10 mM, [KCl] did not significantly increase FluoZin fluorescence in any genotype or at either MeHg concentration. However, at 40 mM, [KCl] application significantly ($p<0.05$) augmented FluoZin fluorescence in all MeHg-treated groups irrespective of genotypes. Further, 40 mM [KCl] significantly ($p<0.05$) increased $[Zn^{2+}]_i$ in G93A mice exposed to 3 ppm MeHg, compared to untreated *wt*.

DISCUSSION

The objective of the present study was to test the concept that exposure to a known environmental neurotoxicant, at levels which were not themselves overtly neurotoxic, would accelerate the onset of the ALS phenotype in a genetically-susceptible mouse. Studies focused on brainstem hypoglossal neuronal soma (NXII), motor neurons which control functions of the tongue including chewing, swallowing, and speaking. In humans, degeneration of NXII motor neurons produces signs and symptoms collectively referred to as bulbar onset ALS (neck and head). This form of ALS is associated with increased morbidity and mortality (Smittkamp et al., 2008). We hypothesized that the common mode of excitotoxic action of MeHg would synergize with that associated with ALS etiology to hasten development of motor dysfunction.

Results of the present study are consistent with the following conclusions. First, chronic exposure to MeHg caused a concentration-dependent shift in rotarod performance to shorten the time to onset of failure, an effect indicative of impairment of motor function, in the genetically-susceptible G93A mice. Second, the SOD1-G93A genotype was associated with elevation in motor neurons of both Ca^{2+} and another non-Ca^{2+} divalent cation- presumably [Zn^{2+}], which is itself neurotoxic. Third, Ca^{2+} and Zn^{2+}-permeable AMPA receptors contributed to enhanced divalent cation levels in G93A motor neurons and MeHg treatment exacerbated this effect.

This is the first unequivocal demonstration of a gene-environment interaction to facilitate development of the ALS phenotype in the G93A mouse. Chronic MeHg exposure in male mice expressing an ALS phenotype (G93A) markedly accelerates the time to onset of hind limb dysfunction. This effect was concentration-dependent. It is

JPET Fast Forward. Published on May 17, 2011 as DOI: 10.1124/jpet.110.174466
This article has not been copyedited and formatted. The final version may differ from this version.

G93A-specific and associated with MeHg exposure. It was not seen in *wt* mice exposed to the highest MeHg concentration (3 ppm) for 120 days. Thus MeHg/G93A interaction was required. Rotarod failure was associated with MeHg accumulation, but MeHg levels in *wt* and G93A mice were equivalent, so the enhancement of motor dysfunction was not due simply to increased accumulation of MeHg in the G93A mice. The concentrations of MeHg used were without effects on generalized function because body weight gain was not reduced by MeHg treatment in either *wt* nor G93A mice. Once rotarod failure ensued, the interval between onset of hind limb dysfunction and paresis was shortened in animals treated with the highest concentration of MeHg. This suggests that even after motor neuron damage begins, MeHg continued to enhance the processes associated with cell death.

ALS pathophysiology coalesces around several mechanisms, including glutamatemediated excitotoxicity (Cluskey and Ramsden, 2001). Included in this is enhanced release of glutamate (Milanese et al., 2010). This causes repetitive firing and dysregulated Ca^{2+} entry leading to cell death, and is a well-known model of brain neurotoxicity (Sinor et al., 2000). MeHg-induced increase in presynaptic $[Ca^{2+}]_i$ is an extensively described mechanism contributing to its neurotoxicity (Limke et al., 2004), as is elevated $[Ca^{2+}]_i$ in spinal cord nerve terminals of the SOD1 mutants (Milanese et al., 2010). Thus a prospective interaction between the MeHg-induced increase in $[Ca^{2+}]_i$, and enhanced glutamate-mediated excitotoxicity in G93A group represented a logical point of intersection for a gene/environment interaction. We determined if hastened onset of ALS-like phenotype in G93A mice is related to the effects of MeHg to increase $[Ca^{2+}]_i$ and the potential contribution of Ca^{2+}-permeable AMPA receptors to this effect. Absolute measurements of $[Ca^{2+}]_i$ were not possible because of differences among

JPET Fast Forward. Published on May 17, 2011 as DOI: 10.1124/jpet.110.174466
This article has not been copyedited and formatted. The final version may differ from this version.

preparations in dye loading efficiency. Consequently, measurements of Fluo-4 fluorescence had to be made in relative terms. After rotarod failure occurred, $[Ca^{2+}]_i$ in brainstem-hypoglossal neuronal soma increased and AMPA receptor antagonists blunted this effect. At a low level of depolarization (10 mM KCl), only the highest MeHg concentration increased Fluo-4 fluorescence. With stronger depolarization (40 mM KCl), a greater level of Fluo-4 fluorescence was seen in all G93A mice irrespective of MeHg treatment. Thus, the increase at low levels of depolarization could reflect a direct effect of MeHg with relatively low contribution of extracellular Ca^{2+}, whereas at higher levels of depolarization, effects of the G93A mutation became more evident. A potentially greater effect of MeHg to increase $[Ca^{2+}]_i$ could have been blunted by the well described ability of MeHg to block voltage-gated Ca^{2+} channels (Shafer and Atchison, 1991; Hajela et al., 2003). The ability of AMPA receptor agonists to replicate the increase in Fluo-4 fluorescence in the G93A group demonstrated that this effect likely resulted from enhanced release of glutamate in the 40 mM KCl group. The ability of AMPA receptor antagonists to counteract the increase in Fluo-4 fluorescence implies that, even in the absence of depolarization, some level of glutamate release is occurring spontaneously in G93A mice.

Increased NXII somal $[Ca^{2+}]$ in the MeHg-treated G93A mice could result from pre- or postsynaptic effects, or a combination of the two. Numerous studies have demonstrated that acute exposure to MeHg increases $[Ca^{2+}]_i$ (Hare et al., 1993; Limke et al., 2003), an effect that should elevate the spontaneous release of neurotransmitters including glutamate (Yuan and Atchison, 2007). MeHg reportedly increases extracellular glutamate levels in rat primary motor cortex (Juárez et al., 2002), a result consistent with increased $[Ca^{2+}]_i$ in presynaptic glutamatergic terminals. We have also

JPET Fast Forward. Published on May 17, 2011 as DOI: 10.1124/jpet.110.174466
This article has not been copyedited and formatted. The final version may differ from this version.

demonstrated that MeHg increased glutamatergic synaptic neurotransmission in brain slices *in vitro* (Yuan and Atchison, 2007). Thus a reasonable expectation is that MeHg treatment could enhance glutamate release secondary to elevation of presynaptic $[Ca^{2+}]_i$.

A TPEN-sensitive pool contributed to the Fluo-4 signal of divalent cations in MeHgtreated animals. We suggest that it is Zn^{2+} based on results of previous studies (Denny and Atchison, 1994) and our results with FluoZin. Elevation of $[Zn^{2+}]_i$ could provide a synergistic effect of MeHg on motor neuron function and degeneration of these neurons in ALS. At higher concentrations, Zn^{2+} is itself cytotoxic. It can enter neurons through Ca^{2+}-permeable AMPA receptors, and it is contained in high concentrations in glutamatergic vesicles. Thus an increased spontaneous release of glutamate could reasonably be expected to increase synaptic levels of Zn^{2+}. MeHg itself liberates a non-Ca^{2+} divalent cation (Denny and Atchison, 1994), potentially contributing further to a releasable Zn^{2+} pool. The extent to which a putative effect of Zn^{2+} contributes to the MeHg/G93A interaction merits further analyses.

Postsynaptic effects of MeHg on glutamate receptors could be an alternate or additional site of action of MeHg. An increased function of Ca^{2+}/Zn^{2+}-permeant AMPA receptors could hasten excitotoxicity in vulnerable motor neurons. The net effect would be to increase postsynaptic $[Ca^{2+}]_i$, secondary to glutamate receptor activation. The response of AMPA receptors to MeHg has not been reported. Consequently we tested whether glutamate agonists could facilitate increases in $[Ca^{2+}]_i$ in MeHg-treated mice. A stimulatory effect of MeHg could result from a) preferential effects to impede expression or function of Ca^{2+}-impermeable AMPA receptors; b) enhanced function of Ca^{2+}-permeable AMPA receptors; or c) an indirect effect to depolarize the membrane

JPET Fast Forward. Published on May 17, 2011 as DOI: 10.1124/jpet.110.174466
This article has not been copyedited and formatted. The final version may differ from this version.

sufficiently to activate NMDA receptors. NXII neurons contain unique combinations of AMPA/KA or NMDA receptors (Essin, 2002). At symptomatic stages of ALS, untreated G93A mice exhibited increased sensitivity to AMPA but not NMDA or KA; MeHg did not change the sensitivity of NMDA receptors. Thus an indirect effect involving NMDA receptor activation can be ruled out. The stimulatory effect of AMPA on Fluo-4 fluorescence was not enhanced further by MeHg, suggesting a lack of a direct effect on the receptor above that seen with the G93A mutation. However, a lack of effect of MeHg to increase Fluo-4 fluorescence further could result from the methodological approach. Methodologically, if the increased $[Ca^{2+}]_i$ elicited by the G93A mutation was of sufficiently high magnitude, the ability of Fluo-4 to report further changes in fluorescence could have been impeded due to dye saturation. Alternatively, a potential increase in glutamate release, or prolonged contact with the AMPA receptor (see below) could have desensitized the receptor, making it incapable of responding to further activation by agonist.

Taking the converse approach we used antagonists to attempt to quell an increase in Fluo-4 fluorescence in the G93A group, as well as a potential enhancement by MeHg should it occur. CNQX reduced Fluo-4 fluorescence and effectively attenuated $[Ca^{2+}]_i$ in G93A and *wt* slices. CNQX produced a more prominent reduction of $[Ca^{2+}]_i$ in the G93A group compared to *wt*. This implies that AMPA receptors contributed significantly to increased $[Ca^{2+}]_i$. This effect was not enhanced by MeHg. Thus AMPA/KA receptors are apparently active and contribute to increased $[Ca^{2+}]_i$. We then used a specific receptor blocker to test if increased $[Ca^{2+}]_i$ was primarily mediated in the G93A group by the Ca^{2+}permeable AMPA receptors. NAS, a polyamine toxin derived from Joro spider venom, binds specifically to GluR2R-lacking AMPA receptors inside

JPET Fast Forward. Published on May 17, 2011 as DOI: 10.1124/jpet.110.174466
This article has not been copyedited and formatted. The final version may differ from this version.

the receptor pore, so that Ca^{2+} influx is prevented (Blaschke et al., 1993). Ca^{2+} was not precluded from entering NXII neurons from *wt* slices, as NAS had no effect on Fluo-4 fluorescence. Conversely, NAS significantly reduced $[Ca^{2+}]_i$ in the G93A group, indicating that a subset of CNQX-sensitive, Ca^{2+}permeable receptors was responsible for increased $[Ca^{2+}]_i$. MeHg enhanced this effect above that of untreated G93A mice in that group, but the MeHg-treated *wt* group did not display NAS sensitivity. As such, MeHg appears to increase $[Ca^{2+}]_i$ of NXII motor neurons by potentiating $[Ca^{2+}]_i$ influx through Ca^{2+}-permeable AMPA receptors. These, in turn, were only found in the G93A group. This once again points to a gene-environmental interaction between the susceptible G93A genotype and MeHg exposure.

In addition to its direct effects on neurons, MeHg could influence motor neuron Ca^{2+} regulation indirectly, particularly by effects on astrocyte function. MeHg accumulates in cortical astrocytes, where it inhibits glutamate uptake through the excitatory amino acid transporter 1 (EAAT-I, also known as GLAST) (Mutkus et al., 2005). The effects of MeHg on brainstem astrocytes have not been examined, but in both patients with ALS, and the mouse model, levels of EAAT-2 are reduced (Barbeito et al., 2004; Boillée et al., 2006). Astrocytes play a critical role in maintaining glutamate homeostasis (see Allen et al., 2002; Aschner et al., 1993; reviewed in Aschner et al., 2000). Thus, a potential increase in the residence time of glutamate in the synaptic cleft due to MeHg-induced disruption of EAAT-2 could theoretically exacerbate glutamate-mediated excitotoxicity of sensitive motor neurons.

In conclusion, our results clearly demonstrate a gene-environment interaction in which MeHg interacts in an organism with a specific gene mutation to hasten the time of onset of development of ALS-like phenotypes. This apparent gene-environment

interaction provides evidence of a potential contribution of MeHg to the development of ALS in genetically-susceptible organisms. MeHg can exhibit a panoply of effects contributing to the acceleration of the ALS phenotype. However in the absence of the synergistic effect of the G93A mutation, the actions of MeHg are not sufficient in and of themselves to induce motorneuron dysfunction over a period of 120 days. Our results support a role for Ca^{2+}permeable AMPA receptors in the MeHg effect. Motor neurons in the G93A mice have an increased abundance of GluR3 mRNA and protein expression coupled with a decrease in protein expression of GluR2 subunits (Tortarolo et al., 2006). This could, in theory, lead to a greater proportion of Ca^{2+}-permeable AMPA receptors which could increase glutamateinduced motor neuron excitotoxicity due to increased $[Ca^{2+}]_i$. Additionally, Yin et al. (2007) demonstrated that intrathecal infusion of NAS reduced motor neuron loss in G93A rats. This effect is presumably due to action on Ca^{2+}-permeable AMPA receptors. A combination of MeHg-induced enhanced response of Ca^{2+}-permeable AMPA receptors coupled with an increase in glutamate release, or decrease in astrocytic EAAT-2 function could predispose motor neurons to excitotoxic damage, thereby unmasking or hastening the onset of ALS in an individual with a known (or, conceivably, an unknown) predilection to the disease. The results of this study also point to the utility of using environmental agents to examine the pathogenesis of other neurodegenerative conditions.

ACKNOWLEDGMENTS: The authors acknowledge the excellent word processing assistance of Elizabeth Anne Hill and Julie Van Raemdonck and graphical assistance of Sarah Metzger. Preliminary reports of portions of this project were presented at the Annual Meetings of the Society of Toxicology, 2010 in Salt Lake City, UT, the 25th International Neurotoxicology Conference, October 12-16, 2008, Rochester, NY and the Society of Neuroscience, November 19, 2008 in Washington DC.

AUTHORS CONTRIBUTIONS

Participated in research design: Atchison, Hajela, Johnson, Parsell, Yuan

Conducted experiments: Chitrakar, Hajela, Johnson, Yuan

Performed data analyses: Atchison, Chitrakar, Hajela, Johnson, Yuan

Wrote or contributed to the writing of the manuscript: Atchison, Hajela, Johnson, Yuan

Other: Atchison acquired funding for research and oversaw the entire project; Parsell was responsible for setting up and maintaining the transgenic mouse colonies.

REFERENCES

Alexander GM, Erwin KL, Byers N, Deitch JS, Augelli BJ, Blankenhorn EP, and Heiman-Patterson TD (2004) Effect of transgene copy number on survival in the SOD1^{G93A} SOD1 transgenic mouse model of ALS. *Brain Res Mol Brain Res* **130**: 7-15.

Allen JW, Shanker G, Tan KH, and Aschner M (2002) The consequences of methylmercury exposure on interactive functions between astrocytes and neurons. *Neurotoxicology.* **23**:755-9.

Arvidson B (1992) Inorganic mercury is transported from muscular nerve terminals to spinal and brainstem motoneurons. *Muscle Nerve* **15**: 1089-94.

Aschner M, Du YL, Gannon M, and Kimelberg HK (1993) Methylmercury-induced alterations in excitatory amino acid transport in rat primary astrocyte cultures. *Brain Res* **602**: 181-6.

Aschner M, Yao CP, Allen JW, and Tan KH (2000) Methylmercury alters glutamate transport in astrocytes. *Neurochem Int* **37**: 199-206.

Bakir F, Damluji SF, Amin-Zaki L, Murtadha M, Khalidi A, Al-Rawi NY, Tikriti S, Dahahir HI, Clarkson TW, Smith JC, and Doherty RA (1973) Methylmercury poisoning in Iraq. *Science* **181**:230-41.

Barbeito LH, Pehar M, Cassina P, Vargas MR, Peluffo H, Viera L, Estevez AG, and Beckman JS (2004) A role for astrocytes in motor neuron loss in amyotrophic lateral sclerosis. *Brain Res Brain Res Rev* **47**:263-74.

Barber TE (1978) Inorganic mercury intoxication reminiscent of amyotrophic lateral sclerosis. *J Occup Med* **20**: 667-9.

Beckman JS, Estévez AG, Crow JP, and Barbeito L (2001) Superoxide dismutase and the death of motoneurons in ALS. *Trends Neurosci* **24**: S15-20.

Bellum S, Thuett KA, Grajeda R, and Abbott LC (2007) Coordination deficits induced in young adult mice treated with methylmercury. *Int J Toxicol* **26**:115-21

Benmohamed R, Arvanites AC, Kim J, Ferrante RJ, Silverman RB, Morimoto RI, and Kirsch DR (2011) Identification of compounds protective against G93A-SOD1 toxicity for the treatment of amyotrophic lateral sclerosis. *Amyotroph Lateral Scler* **12**:87-96.

Blaschke M, Keller BU, Rivosecchi R, Hollmann M, Heinemann S, and Konnerth A (1993) A single amino acid determines the subunit-specific spider toxin block of alpha-amino-3 hydroxy-5-methylisoxazole-4-propionate/kainate receptor channels. Proc Natl Acad Sci USA **90**:6528-32.

Boillée S, Vande Velde C, and Cleveland DW (2006) ALS: A disease of motor neurons and their nonneuronal neighbors. *Neuron* **52**:39-59.

Brown RH Jr. (1995) Amyotrophic Lateral Sclerosis: Recent insights from genetics and transgenic mice *Cell* **80**:687-92

Cluskey S and Ramsden DB (2001) Mechanisms of neurodegeneration in amyotrophic lateral sclerosis. *Mol Pathol* **54**: 386-92.

Denny MF, Hare MF, and Atchison WD (1993) Methylmercury alters intrasynaptosomal concentrations of endogenous polyvalent cations. *Toxicol Appl Pharmacol* **122:** 222-32.

Denny MF and Atchison WD (1994) Methylmercury-induced elevations in intra-synaptosomal zinc concentrations: an ^{19}F-NMR study. *J Neurochem* **63:** 383-6.

DePaul R, Abbs JH, Caligiuri M, Gracco VL, and Brooks BR (1988) Hypoglossal, trigeminal, and facial motoneuron involvement in amyotrophic lateral sclerosis. *Neurology* **38**:281-3.

Essin K, Nistri A, and Magazanik L (2002) Evaluation of GluR2 subunit involvement in AMPA receptor function of neonatal rat hypoglossal motoneurons. *Eur J Neurosci* **15**: 1899906.

Grosskreutz J, Van Den Bosch L, and Keller BU (2010) Calcium dysregulation in amyotrophic lateral sclerosis. *Cell Calcium* **47**:165-74.

Gruzman A, Wood WL, Alpert E, Prasad MD, Miller RG, Rothstein JD, Bowser R, Hamilton R, Wood TD, Cleveland DW, Lingappa VR, and Liu J (2007) Common molecular signature in SOD1 for both sporadic and familial amyotrophic lateral sclerosis. *Proc Natl Acad Sci USA* **104**:12524-9.

Gurney ME, Pu H, Chiu AY, Dal Canto MC, Polchow CY, Alexander DD, Caliendo J, Hentati A, Kwon YW, Deng HX, Chen W, Zhai P, Sufit RL, and Siddique T (1994) Motorneuron degeneration in mice that express a human Cu, Zn superoxide dismutase. *Science* **264:** 1772-5.

Haley RW (2003) Excess incidence of ALS in young Gulf War veterans. *Neurology* **61**: 750-6.

Hajela RK, Peng SQ, and Atchison WD (2003) Comparative effects of methylmercury and Hg^{2+} on human neuronal N- and R-type high-voltage activated calcium channels transiently expressed in human embryonic kidney 293 cells. *J Pharmacol Exp Ther* **306**:1129-36.

Hare MF, McGinnis KM, and Atchison WD (1993) Methylmercury increases intracellular concentrations of Ca^{++} and heavy metals in NG108-15 cells. *J Pharmacol Exp Ther* **266:** 1626-35.

Horner RD, Kamins KG, Feussner JR, Grambow SC, Hoff-Lindquist J, Harati Y, Mitsumoto H, Pascuzzi R, Spencer PS, Tim R, Howard D, Smith TC, Ryan MA,

Coffman CJ, and Kasarskis EJ (2003) Occurrence of amyotrophic lateral sclerosis among Gulf War veterans. *Neurology* **61**: 742-9.

Institute of Medicine of the National Academies (2006) Amyotrophic Lateral Sclerosis in Veterans: Review of the Scientific Literature, Board on Population Health and Public Health Practice, Released 11/ 6/2006. http://books.nap.edu/openbook.php? record_ id=1175.

Juárez BI, Martínez ML, Montante M, Dufour L, García E, and Jiménez-Capdeville ME (2002) Methylmercury increases glutamate extracellular levels in frontal cortex of awake rats. *Neurotoxicol Teratol* **24:** 767-71.

Kabashi E, Valdmanis PN, and Dion P (2008) TARDBP mutations in individuals with sporadic and familial amyotrophic lateral sclerosis. *Nat Genet* **40**:572–4.

Kamel F, Umbach DM, Stallone L, Richards M, Hu H, and Sandler DP (2008) Association of lead exposure with survival in amyotrophic lateral sclerosis. *Environ Health Perspect* **116**: 943-7.

Karsarkis EJ, Scarlata D, Hill R, Fuller C, Stambler N, and Cedarbaum JM (1999) A retrospective study of percutaneous endoscopic gastrostomy in ALS patients during the BDNF and CNTF trials. *J Neurol Sci* **169:** 118-25.

Kawahara Y, Ito K, Sun H, Aizawa H, Kanazawa I, and Kwak S (2004) Glutamate receptors: RNA editing and death of motor neurons. *Nature* **427**: 801.

Kwak S, Hideyama T, Yamashita T, and Aizawa H (2010) AMPA receptor-mediated neuronal death in sporadic ALS. *Neuropathology* **30**: 182-8.

Le W, Chen S, and Jankovic J (2009) Etiopathogenesis of Parkinson Disease: a new beginning? *Neuroscientist* **15**: 28-35.

Limke TL, Otero-Montañez JK, and Atchison WD (2003) Evidence for interactions between intracellular calcium stores during methylmercury-induced intracellular calcium dysregulation in rat cerebellar granule neurons. *J Pharmacol Exp Ther* **304**: 949-58.

Limke TL, Heidemann SR, and Atchison WD (2004) Disruption of intraneuronal divalent cation regulation by methylmercury: are specific targets involved in altered neuronal development and cytotoxicity in methylmercury poisoning. *Neurotoxicology* **25**: 741-60.

Migliore L and Coppedè F (2009) Genetics, environmental factors and the emerging role of epigenetics in neurodegenerative diseases. *Mutat Res* **667**: 82-97.

Milanese M, Zappettini S, Onofri F, Musazzi L, Tardito D, Bonifacino T, Messa M, Racagni G, Usai C, Benfenati F, Popoli M, and Bonanno G. (2011) Abnormal exocytotic release of glutamate in a mouse model of amyotrophic lateral sclerosis. *J Neurochem* **116**:1028-42.

Mitchell JD (2000) Amyotrophic lateral sclerosis: toxins and environment. *Amyotroph Lateral Scler Other Motor Neuron Disord.* **1**: 235-50.

Møller-Madsen B (1991) Localization of mercury in CNS of the rat III. Oral administration of methylmercuric chloride (CH_3HgCl). *Fundam Appl Toxicol* **16**: 172-87.

Mutkus L, Aschner JL, Syversen T, and Aschner M (2005) Methylmercury alters the in vitro uptake of glutamate in GLAST- and GLT-1-transfected mutant CHO-K1 cells. *Biol Trace Elem* **107**:231-45.

Newland MC and Rasmussen EB (2000) Aging unmasks adverse effects of gestational exposure to methylmercury in rats. *Neurotoxicol Teratol* **22**:819-28.

Newland MC, Reile PA, and Langston JL (2004) Gestational exposure to methylmercury retards choice in transition in aging rats. *Neurotoxicol Teratol* **26**:179-94.

Prasad KN, Cole WC, and Kumar B (1999) Multiple antioxidants in the prevention and treatment of Parkinson's disease. *J Am Coll Nutr* **18**: 413-23.

Rembach A, Turner BJ, Bruce S, Cheah IK, Scott RL, Lopes EC, Zagami CJ, Beart PM, Cheung NS, Langford SJ, and Cheema SS (2004) Antisense peptide nucleic acid targeting GluR3 delays disease onset and progression in the SOD1 G93A mouse model of familial ALS. J *Neurosci Res* **77**:573-82.

Rowland LP and Shneider NA (2001) Amyotrophic lateral sclerosis. *N Engl J Med* **11**: 11312.

Shafer TJ, and Atchison WD (1991) Methylmercury blocks N- and L-type Ca^{++} channels in nerve growth factor-differentiated pheochromocytoma (PC12) cells. *J Pharmacol Exp Ther* **258**:149-57.

Sinor JD, Du S, Venneti S, Blitzblau RC, Leszkiewicz DN, Rosenberg PA, and Aizenman E (2000) NMDA and glutamate evoke excitotoxicity at distinct cellular locations in rat cortical neurons in vitro. *J Neurosci* **20:** 8831-7.

Shmist YA, Kamburg R, Ophir G, Kozak A, Shneyvays V, Appelbaum YJ, and Shainberg A (2005) N,N,N',N'-tetrakis(2-pyridylmethyl)-ethylenediamine improves myocardial protection against ischemia by modulation of intracellular Ca^{2+} homeostasis. *J Pharmacol Exp Ther* **313:** 1046-57.

Smittkamp SE, Brown JW, and Stanford JA (2008) Time-course and characterization of orolingual motor deficits in B6SJL-Tg(SOD1-SOD1^{G93A})1Gur/J mice. *Neuroscience* **151**: 613-21.

Sreedharan J, Blair IP, Tripathi VB, Hu X, Vance C, Rogelj B, Ackerley S, Durnall JC, Williams KL, Buratti E, Baralle F, de Belleroche J, Mitchell JD, Leigh PN, Al-Chalabi A, Miller CC, Nicholson G, and Shaw CE (2008) TDP-43 mutations in familial and sporadic amyotrophic lateral sclerosis. *Science* **319**:1668-72.

Stern AH and Korn LR (2001) How useful is linear regression analysis in detecting the existence of dose-response relationships in large-scale epidemiologic studies when only a fraction of the population is sensitive? The case of methylmercury. *Regul Toxicol Pharmacol* **33**: 29-36.

Stern S, Cox C, Cernichiari E, Balys M, and Weiss B (2001) Perinatal and lifetime exposure to methylmercury in the mouse: blood and brain concentrations of mercury to 26 months of age. *Neurotoxicology* **22**:467-77.

Swash M (2000) Nature and nurture in ALS. *Amyotroph Lateral Scler* **1**: 223.

Synofzik M, Fernández-Santiago R, Maetzler W, Schöls L, and Andersen PM (2010) The human G93A SOD1 phenotype closely resembles sporadic amyotrophic lateral sclerosis. *J Neurol Neurosurg Psych* **7**:764-7.

Tateno M, Sadakata H, Tanaka M, Itohara S, Shin RM, Miura M, Masuda M, Aosaki T, Urushitani M, Misawa H, and Takahashi R (2004) Calcium-permeable AMPA receptors promote misfolding of mutant SOD1 protein and development of amyotrophic lateral sclerosis in a transgenic mouse model. *Hum Mol Genet* **13:** 2183-96

.

Tortarolo M, Grignaschi G, Calvaresi N, Zennaro E, Spaltro G, Colovic M, Fracasso C, Guiso G, Elger B, Schneider H, Seilheimer B, Caccia S, and Bendotti C (2006) Glutamate AMPA receptors change in motor neurons of SOD1 transgenic mice and

their inhibition by a noncompetitive antagonist ameliorates the progression of amytrophic lateral sclerosis-like disease. *J Neurosci Res* **83:** 134-46.

Weiss B, Stern S, Cox C, and Balys M (2005) Perinatal and lifetime exposure to methylmercury in the mouse: behavioral effects. *Neurotoxicology* **26**: 675-90.

Yin HZ, Tang DT, Weiss JH (2007) Intrathecal infusion of a Ca(2+)-permeable AMPA channel blocker slows loss of both motor neurons and of the astrocyte glutamate transporter, GLT-1 in a mutant SOD1 rat model of ALS. *Exp Neurol.* ***207***:177-85.

Yuan Y, and Atchison WD (2007) Methylmercury-induced increase of intracellular Ca^{2+} increases spontaneous synaptic current frequency in rat cerebellar slices. *Mol Pharmacol* **71**: 1109-21.

FOOTNOTES This study was supported by the following grants from the National Institute of Environmental Health Sciences: [5T32 ES007255], [R21ES014357], and [R01ES03299] including an ARRA supplement to this grant. Alisha Chitrakar was supported in part by a Summer Undergraduate Research Fellowship from the American Society of Pharmacology and Experimental Therapeutics and was the recipient of a Pfizer Undergraduate Research Award from the Society of Toxicology (2010) for her role on the project.

JPET Fast Forward. Published on May 17, 2011 as DOI: 10.1124/jpet.110.174466
This article has not been copyedited and formatted. The final version may differ from this version.

FIGURE LEGENDS

Figure 1. Time course of experimental design for MeHg exposure, rotarod training and development of ALS phenotype. After weaning (PND 21) and genotyping, cohorts of male G93A and *wt* mice were randomly assigned to groups treated with 0, 1, or 3 ppm of MeHg. Mice received MeHg free-choice via drinking water starting on PND29 and continuing until sacrifice.

Figure 2. Comparison of mean body weight during chronic exposure of SOD1G93A and *wt* male mice to MeHg. (A) Time course of changes in body weight in untreated G93A male mice (■) or those exposed to 1 (□) or 3 ppm (▼) MeHg and *wt* mice exposed to 3 ppm MeHg (●). (B) *Wt* males were exposed to 0 ppm (□) or 3 ppm (●) MeHg. All values represent the mean ± SEM, *n* = 14 mice/treatment/genotype. The asterisk (*) indicates a value significantly different from *wt* ($p<0.05$).

Figure 3. Chronic MeHg exposure hastened disease onset and progression in SOD1G93A mice. (A) Time course of onset of rotarod failure in, 0 (■) , 1 (□) or 3 ppm (▼) MeHg-treated G93A and 3 ppm MeHg-treated *wt* (●). 50% Cumulative failure of the population occurred at 84 and 91 days (arrows) compared to 104 days for the control group; no failure occurred in *wt* mice. (B) Mean time of onset and progression of paralytic ALS-like phenotypes in G93A mice. The asterisk (*) depicts a significant ($p<0.05$) difference between untreated and treated G93A mice: A concentration-dependence occurred to time of onset but not time to progression. All values represent

mean ± SEM, *n* = 14 mice/treatment/genotype; Key: W3= *wt* 3 ppm; G0= G93A 0 ppm; G1= G93A 1 ppm; G3= G93A 3 ppm.

Figure 4. Chronic MeHg exposure, increased $[Ca^{2+}]_i$ Fluo-4 fluorescence in G93A slices following incubation with TPEN and puff application of [KCl]. (A) Membrane depolarization with [KCl] (40 mM) increased Fluo-4 Ca^{2+} fluorescence in NXII nuclei of G93A mice. (B) N,N,N',N'-Tetrakis (pyridylmethyl) ethylenediamine (TPEN) significantly reduced Fluo-4 fluorescence. All values represent mean ± SEM, *n* = 8 mice/treatment/genotype; ($p<0.05$). The asterisk (*) indicates a significant difference between *wt* and G93A mice ($p<0.05$); the cross (†) indicates a significant difference between MeHg-treated and untreated G93A mice following puff application of [KCl] ($p<0.05$); $^{a}p<0.05$ differences between TPEN-treated and untreated slices; the plus (+) indicates a significant difference between [KCl] at 10 mM and 40 mM in TPEN-treated and untreated slices. Key: W0= *wt* 0 ppm; W3= *wt* 3 ppm; G0= G93A 0 ppm; G1= G93A 1 ppm; G3= G93A 3 ppm.

Figure 5. Pharmacological identification of glutamate receptors regulating $[Ca^{2+}]_i$ in XII nuclei in *Wt* and G93A mice. Application of AMPA increased Ca^{2+} entry through AMPA/KA receptors. All values represent mean ± SEM, *n* = 8 mice/treatment/genotype. *$p<0.05$ difference between genotypes; $^{‡}p<0.05$ differences between treated *wt* and G93A mice slices. Key: W0= *wt* 0 ppm; W3= *wt* 3 ppm; G0= G93A 0 ppm; G1= G93A 1 ppm; G3= G93A 3 ppm.

Figure 6. Pharmacological identification of AMPA receptor subunits regulating $[Ca^{2+}]_i$ in XII nuclei of *Wt* and G93A male mice. Application of glutamate receptor

JPET Fast Forward. Published on May 17, 2011 as DOI: 10.1124/jpet.110.174466
This article has not been copyedited and formatted. The final version may differ from this version.

antagonists decreased Ca^{2+} entry via AMPA-type receptors including those presumably lacking the GluR2 subunit (NAS-sensitive). All values represent the mean ± SEM, *n* = 8 mice/ treatment/genotype; The asterisk (*) depicts a significant difference ($p<0.05$) between genotypes. The cross (†) depicts a significant difference ($p<0.05$) between MeHg-treated and untreated G93A mice; Dunnett's *posthoc* tests. Key: W0= *wt* 0 ppm; W3= *wt* 3 ppm; G0= G93A 0 ppm; G1= G93A 1 ppm; G3= G93A 3 ppm.

Figure 7. Chronic MeHg exposure, increased FluoZin fluorescence in G93A slices following puff application of [KCl]. (A) Membrane depolarization with [KCl] (40 mM) increased FluoZin (Zn^{2+}) fluorescence in NXII nuclei of treated mice irrespective of genotypes. All values represent the mean ± SEM, *n* = 8 mice/treatment/genotype; ($p<0.05$). The asterisk (*) indicates a significant difference between untreated *wt* mice ($p<0.05$); the cross (†) indicates a significant difference between MeHg-treated and untreated G93A mice following puff application of [KCl] ($p<0.05$). Key: W0= *wt* 0 ppm; W3= *wt* 3 ppm; G0= G93A 0 ppm; G1= G93A 1 ppm; G3= G93A 3 ppm.

JPET Fast Forward. Published on May 17, 2011 as DOI: 10.1124/jpet.110.174466
This article has not been copyedited and formatted. The final version may differ from this version.

Table 1: Total tissue Hg concentration following chronic methylmercury exposure of hSOD1^{G93A} and wt male mice a

Genotypes and MeHg concentration [ppm]		Blood [ppm][1, 3]	Brainstem [ppm]
hSOD1^{G93A}	0	N.D.[2]	N.D.
hSOD1^{G93A}	1	4.1 ± 0.6	3.6 ± 0.6
hSOD1^{G93A}	3	9.9 ± 2.3	9.1 ± 1.8
Wild type	3	9.7 ± 2.0	9.1 ± 2.4

[1]Data are expressed as mean ± SEM with n = 10 mice/treatment/genotype.
[2]ND = not detectable;
[3]100 µl of blood were used for total mercury assay.

Figure 1

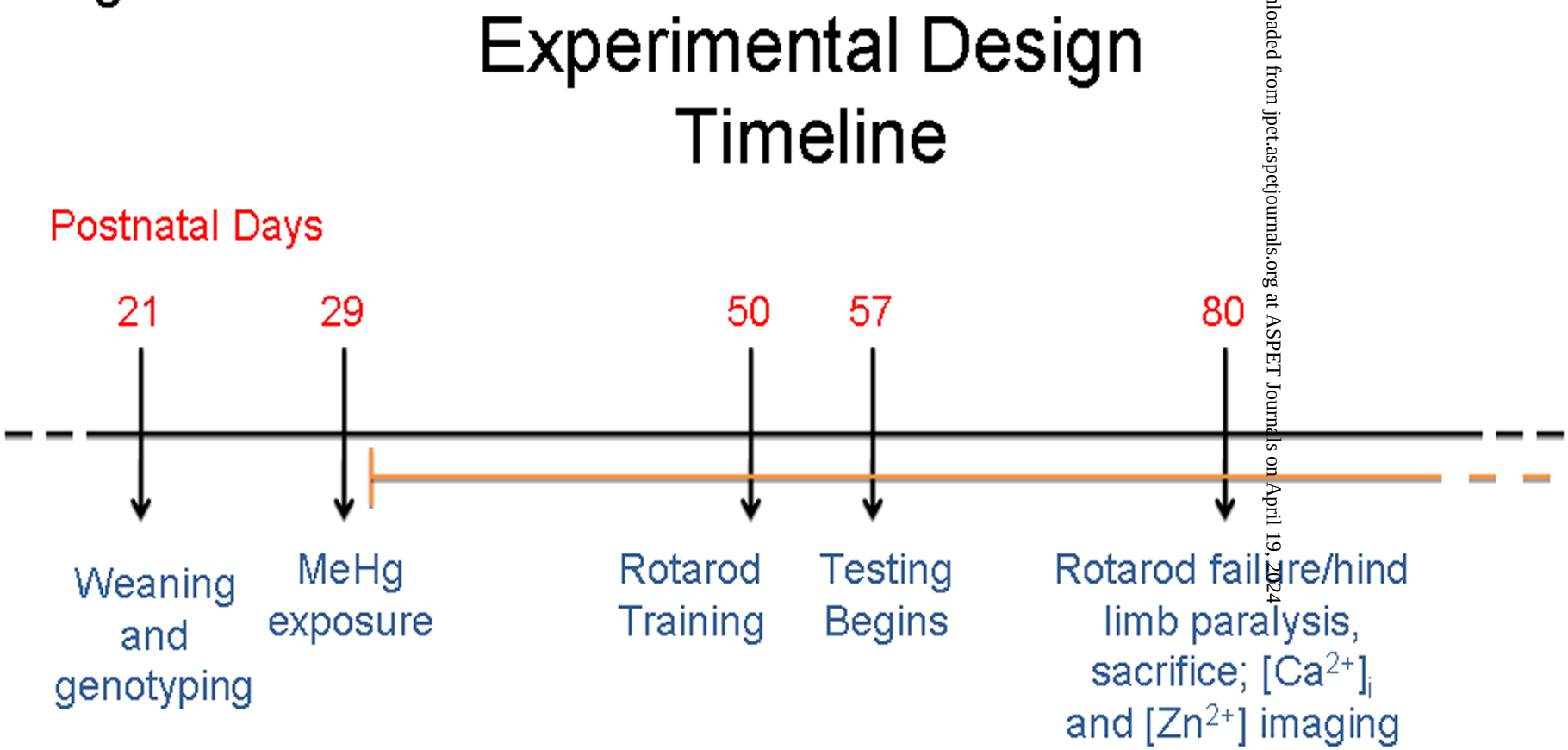

FIGURE 2

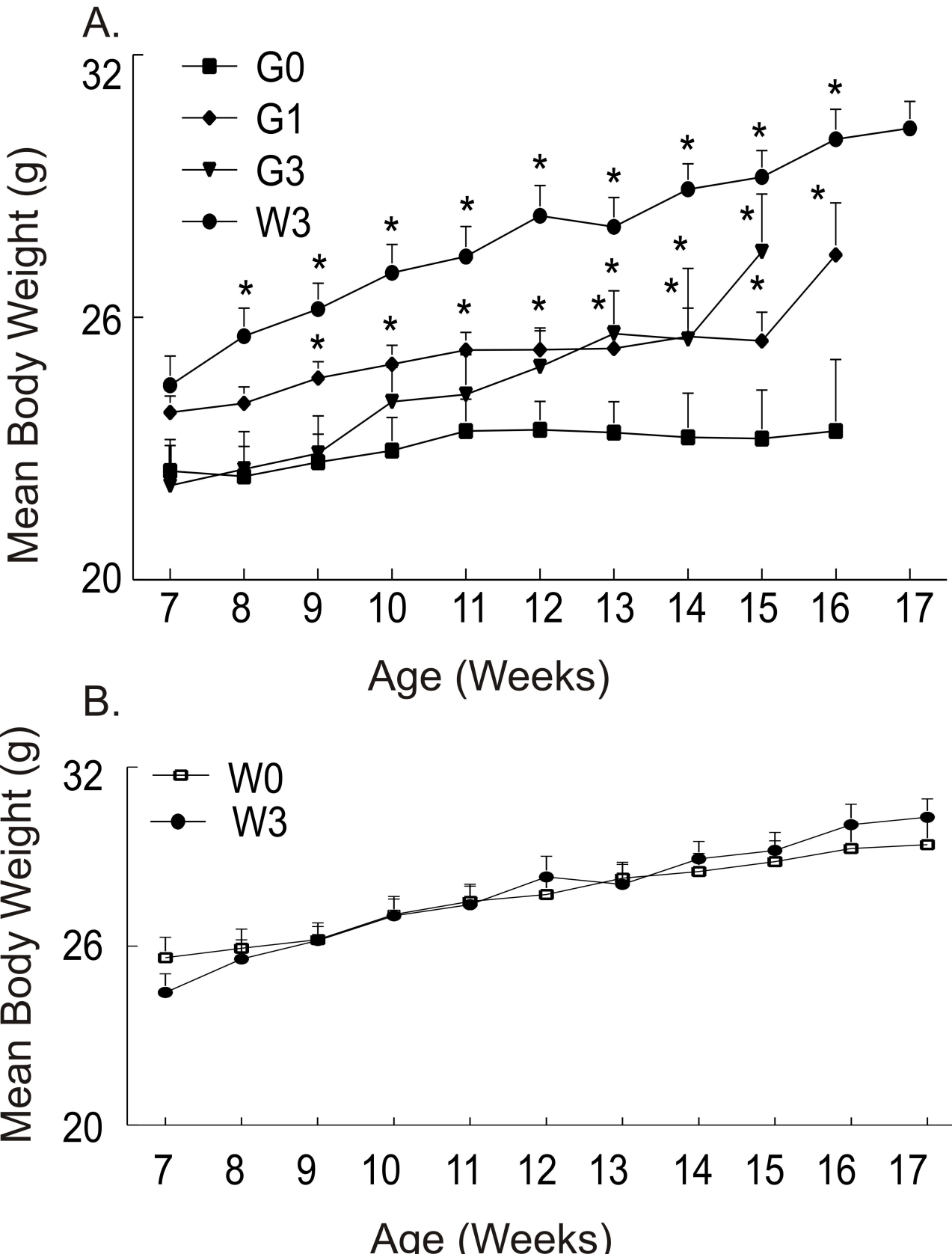
A.
32
26
20
G0
G1
G3
W3
Mean Body Weight (g)
7
8
9
10
11
12
13
14
15
16
17
Age (Weeks)
B.
32
26
20
W0
W3
Mean Body Weight (g)
7
8
9
10
11
12
13
14
15
16
17
Age (Weeks)

FIGURE 3

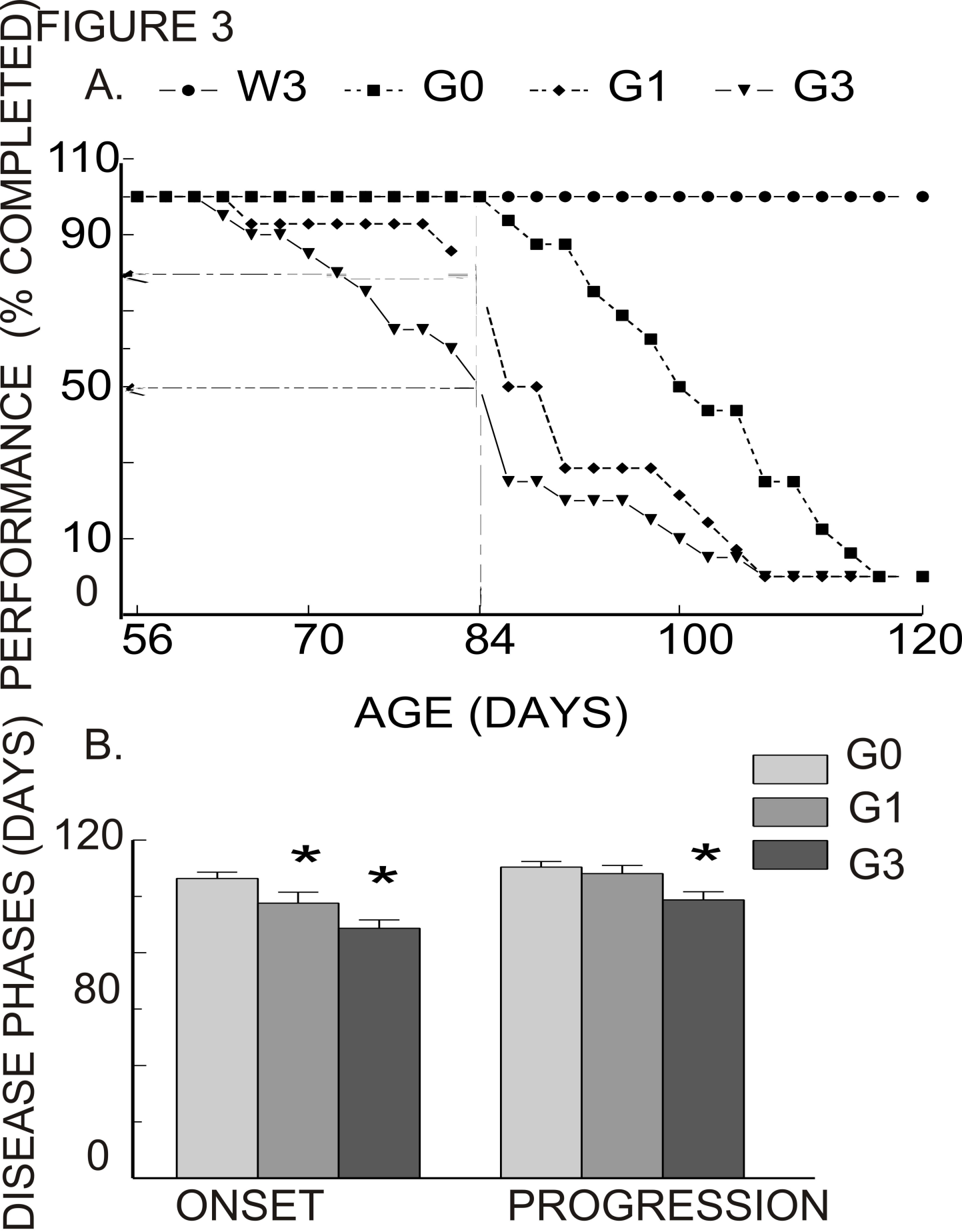
A.
W3
G0
G1
G3
110
90
50
10
0
PERFORMANCE (% COMPLETED)
56
70
84
100
120
AGE (DAYS)
B.
G0
G1
G3
120
80
0
DISEASE PHASES (DAYS)
*
*
*
ONSET
PROGRESSION

FIGURE 4

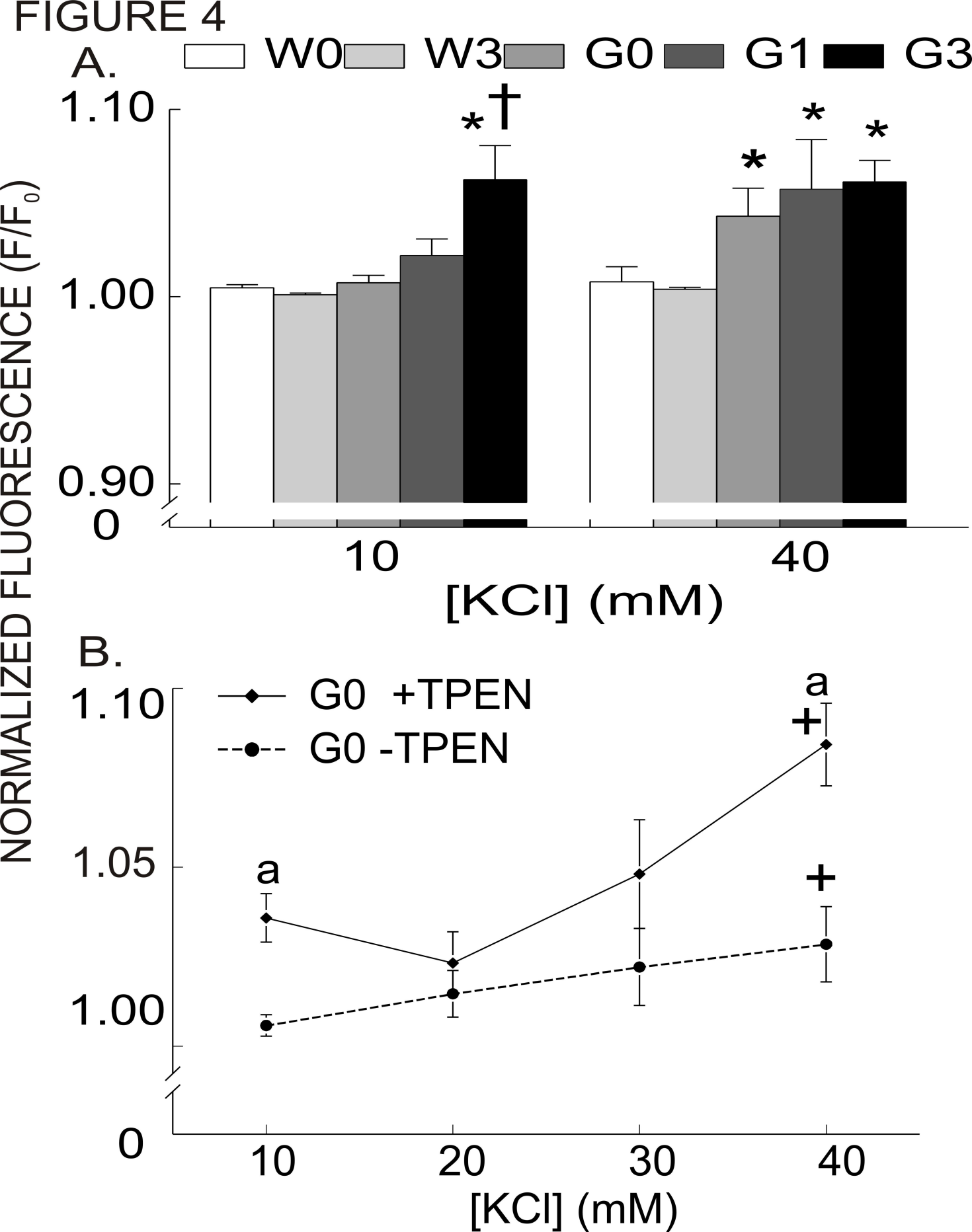
A.
W0
W3
G0
G1
G3
1.10
1.00
0.90
0
NORMALIZED FLUORESCENCE (F/F0)
*†
*
*
*
10
40
[KCl] (mM)
B.
G0 +TPEN
G0 -TPEN
1.10
1.05
1.00
0
a
a
+
+
10
20
30
40
[KCl] (mM)

Figure 5

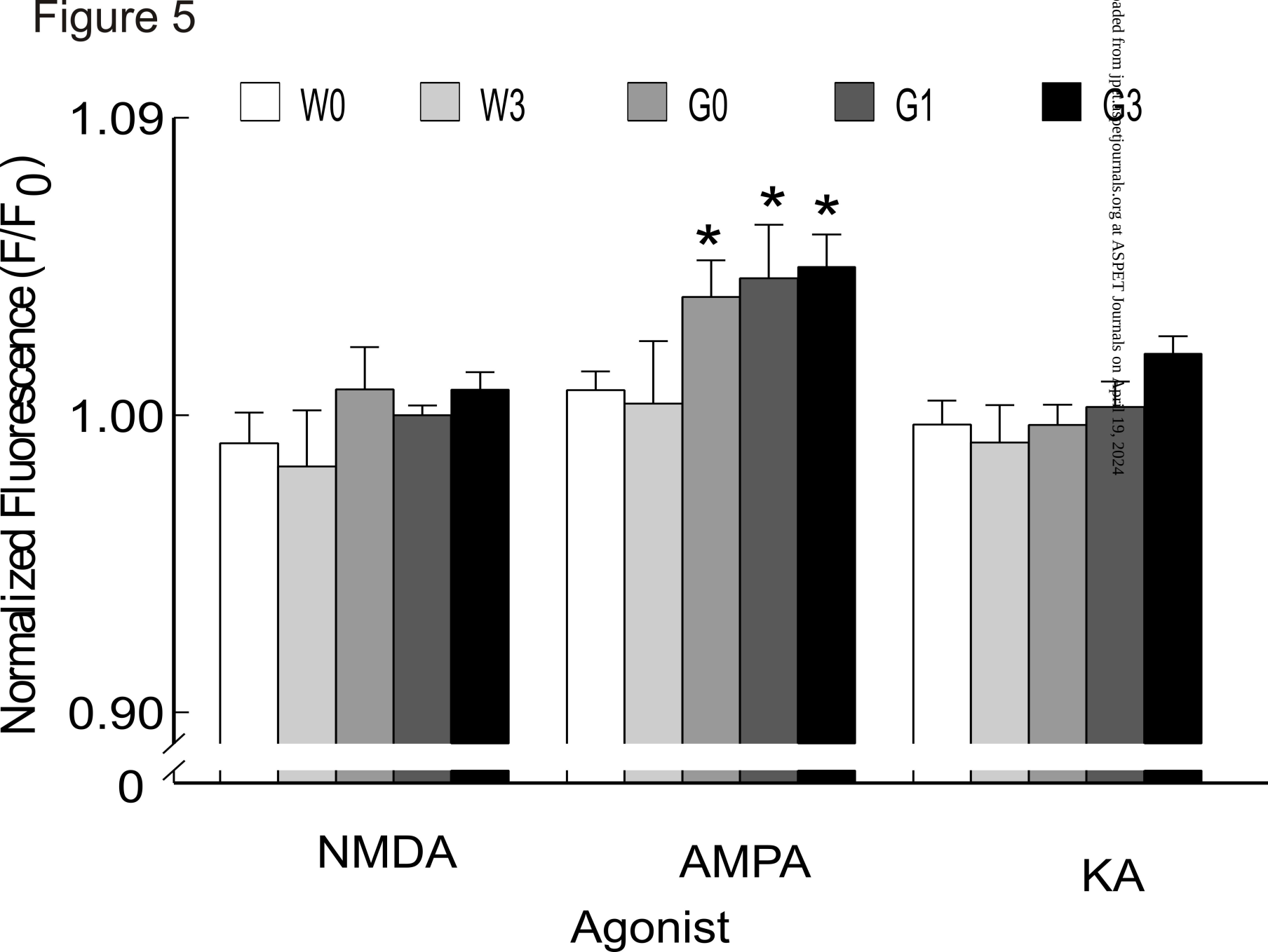

Figure 6

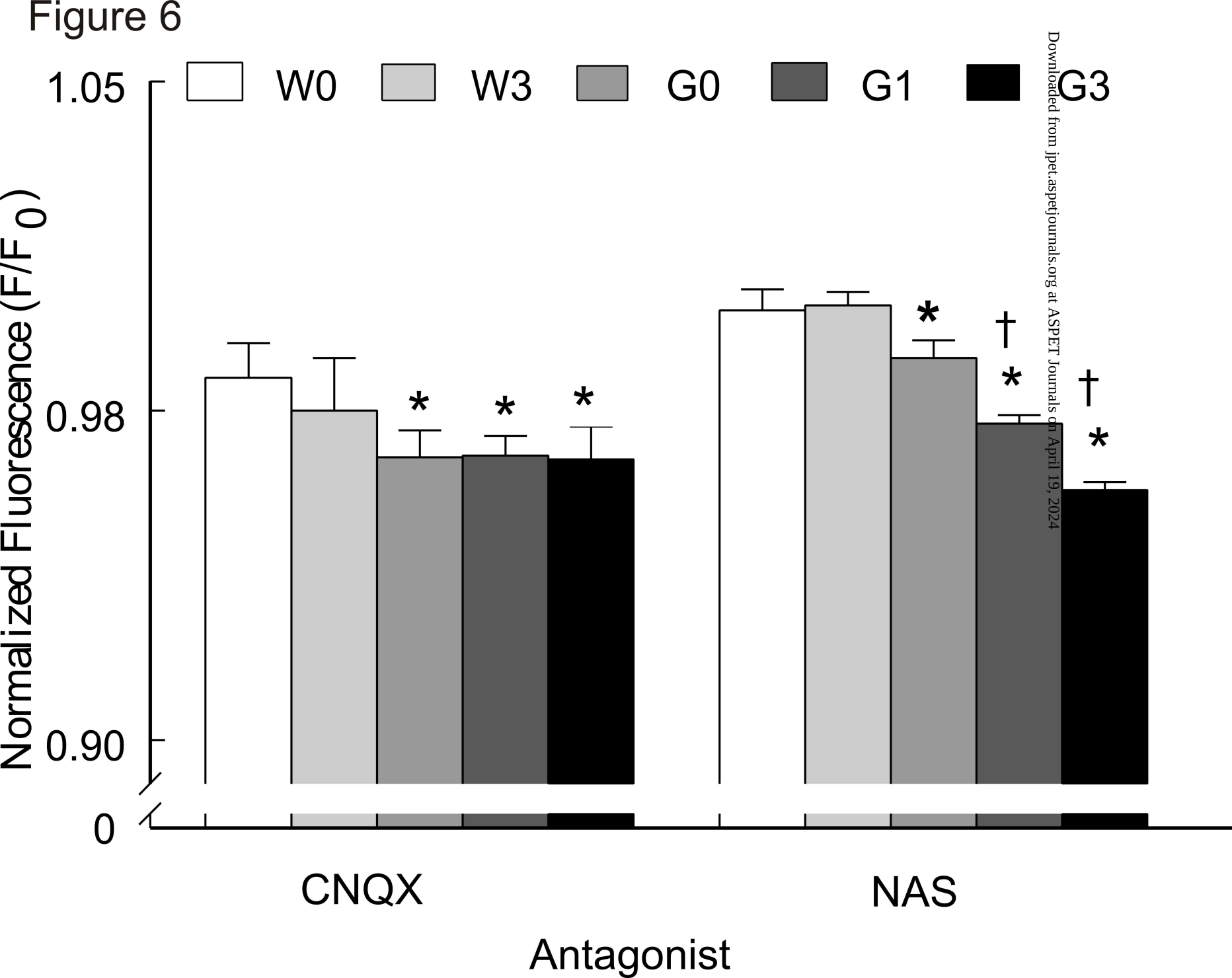

Figure 7